



## Research article

Characterization of whey protein-based films incorporated with natamycin and nanoemulsion of  $\alpha$ -tocopherolCamilo Agudelo-Cuartas<sup>a</sup>, Diana Granda-Restrepo<sup>a,\*</sup>, Paulo J.A. Sobral<sup>b,c</sup>, Hugo Hernandez<sup>d</sup>, Wilson Castro<sup>e</sup><sup>a</sup> BIOALI, Research Group, Department of Food, Faculty of Pharmaceutical and Food Sciences, University of Antioquia, Cl 67 No. 53 - 108 Medellín, Colombia<sup>b</sup> Department of Food Engineering, College of Animal Science and Food Engineering, University of Sao Paulo, Av. Duque de Caxias North, 225, 13635-900, Pirassununga, SP, Brazil<sup>c</sup> Food Research Center (FoRC), University of São Paulo, Rua do Lago, 250, Semi-industrial Building, Block C; 05508-080, São Paulo SP, Brazil<sup>d</sup> ForsChem Research, Cl 34 No. 63B-72, 050030 Medellín, Colombia<sup>e</sup> Facultad de Ingeniería de Industrias Alimentarias, Universidad Nacional de Frontera. Av. San Hilarión N° 101, Sullana, Piura, Perú

## ARTICLE INFO

## Keywords:

Food science  
Food technology  
Materials science  
Nanotechnology  
Nanoemulsion  
Whey protein-based films  
Active packaging  
 $\alpha$ -tocopherol  
Natamycin

## ABSTRACT

Food packaging materials are commonly derived from petroleum that increases global contamination; this raises the interest to evaluate raw material from renewable sources such as whey protein for the development of packaging materials, especially to produce active films. This research aimed to evaluate whey protein-based film properties when natamycin, nanoemulsified  $\alpha$ -tocopherol, or both were added. An oil-in-water (O/W) nanoemulsion of antioxidant ( $\alpha$ -tocopherol) was prepared by microfluidization technique. Four films were prepared with different levels of natamycin and nanoemulsified  $\alpha$ -tocopherol and were characterized in terms of physicochemical, mechanical, optical-properties, water vapor barrier, FTIR, microstructure, antioxidant and antimicrobial activity. The natamycin, nanoemulsified  $\alpha$ -tocopherol, or both did not modify the moisture content of the films. Moreover lead to a significant reduction of tensile strength and elastic modulus, while presenting growth in the elongation at break. Film opacity, the total color difference, the UV-Vis light barrier, and the water vapor permeability values increased when compounds were incorporated into the film. The microstructure studies showed uniformly distributed porosity throughout the films. The addition of nanoemulsified  $\alpha$ -tocopherol into whey protein-based films provoked antioxidant activity and the addition of natamycin produced films with effectivity against *C. albicans*, *P. chrysogenum*, and *S. cerevisiae*, allowing develop a material appropriate for use as active food packaging.

## 1. Introduction

Up to 2015, around 6300 million tons of plastic waste has been produced, 79% are discarded, 12% are burned, and only 9% are recycled (Zhao et al., 2018). Landfill and incineration are traditional methods to handle plastic waste leading to a negative environmental impact (Khalil et al., 2016). This context has led to the implementation of laws on the reasonable use of plastic materials, as in the case of Europe regarding the reduction of usage of light plastic bags with the Directive (EU) 2015/720. The growing worldwide problem of the contamination of petroleum-based plastics and the need to generate new materials as alternatives for food packaging have opened a field of research for the

development of biodegradable containers from renewable sources (Dammak et al., 2017).

An alternative to petroleum-based plastic could be materials based on biopolymers derived from animal sources such as collagen (Cazón et al., 2017), gelatin (Dammak et al., 2017), chitosan (Ahmed and Ikram., 2016; Cazón et al., 2017), chitosan and gelatin (Bonilla and Sobral., 2016; Pérez-Córdoba et al., 2018), whey proteins isolated and concentrated whey (Ghadetaj et al., 2018; Schmid et al., 2017); or from vegetal sources, such as Zein (Oymaci and Altinkaya., 2016), cellulose (Lavoine et al., 2016), starch (Ollé-Resa, Gerschenson, and Jagus., 2014a, 2016), and gluten (Fajardo et al., 2010), among others.

The whey proteins have been of great interest because, at present, the world manufacture of cheese whey annually is around  $1.8\text{--}1.9 \times 10^8$  tons

\* Corresponding author.

E-mail address: [diana.granda@udea.edu.co](mailto:diana.granda@udea.edu.co) (D. Granda-Restrepo).<https://doi.org/10.1016/j.heliyon.2020.e03809>

Received 20 August 2019; Received in revised form 16 January 2020; Accepted 16 April 2020

2405-8440/© 2020 The Authors. Published by Elsevier Ltd. This is an open access article under the CC BY-NC-ND license (<http://creativecommons.org/licenses/by-nc-nd/4.0/>).

**Table 1.** Formulation of FFS for WPC films loaded with active compounds. F0: Film without active compounds (Control film); F1: 2%  $\alpha$ -TOC – 0 ppm NAT; F2: 0%  $\alpha$ -TOC – 300 ppm NAT; F3: 2%  $\alpha$ -TOC – 300 ppm NAT.

Film	Component	F0	F1	F2	F3
Composition	$\alpha$ -TOC (%)	0	2	0	2
	NAT (ppm)	0	0	300	300
Formulation of FFS (% w/w)	WPC	10.0	10.0	10.0	10.0
	Distilled water	85.0	52.5	85.0	52.5
	Glycerol	5.0	5.0	5.0	5.0
	Nanoemulsion	0	32.5	0	32.5
	NAT	0	0	0.0123	0.0123

(Zhou et al., 2019). The predominant proteins in whey are  $\alpha$ -lactalbumin and  $\beta$ -lactoglobulin, with a high nutritional value representing about 50% and 20% of the total protein content, these proteins can form emulsions, foams, gels, and a high potential to form biopolymer-based materials for food applications (Ghadetaj et al., 2018; Ozer et al., 2016; Schmid et al., 2018; Shokri and Ehsani, 2017). The packaging materials made with these proteins are also edible and biodegradable, presenting an excellent barrier to gases compared with conventional plastics (Oymaci and Altinkaya, 2016). Moreover, these materials can serve as vehicles of bioactive compounds allowing the development of active food packaging (Atares and Chiralt, 2016).

Antimicrobial substances have been studied as fungicides, natural extracts, enzymes, bacteriocins, and organic acids for their application in biodegradable films (Altenhofen et al., 2012; Pintado et al., 2010). A cause of food spoiling corresponds to the growth of microorganisms, such as molds and yeasts, which compromise food stability and threaten consumer safety because they can produce mycotoxins (Moatsou et al., 2015). Natamycin is a natural additive obtained by the fermentation of the bacterium *Streptomyces natalensis*; it is a natural antifungal agent and is widely used to prevent contamination by yeasts and molds in different food products. Natamycin has advantages as an additive because it does not have color, odor, and taste; also, the Food and Drug Administration has considered natamycin as a recognized product as safe and the European Union as a natural preservative (E235). This fungicide of the polyene macrolide group acts on the ergosterol of the cell membrane and can be used for cheese surface treatment (Ramos et al., 2012; Ollé-Resa, Gerschenson, and Jagus, 2014a; Moatsou et al., 2015).

The lipid oxidation is another cause of food deterioration and has effects on bad odors, color loss, harmful compounds, and the development of off-flavors. The  $\alpha$ -tocopherol is generally accepted as a soluble lipid antioxidant it is recommended for use in foods containing fats, oils and has been used in edible films by Martins et al. (2012) in chitosan, Martelli et al. (2017) in carboxymethyl cellulose, Noronha et al. (2014) in methylcellulose, Shokri and Ehsani (2017) in whey protein concentrate and Bonilla and Sobral (2016); Pérez-Córdoba et al. (2017, 2018) in gelatin-chitosan.

Tocopherols were cataloged as substances generally GRAS for food products by the Code of Federal Regulations; hence the use of  $\alpha$ -tocopherol as an antioxidant natural has increased the interest in protecting and extending the shelf life in food (Granda-Restrepo et al., 2009; Shokri and Ehsani, 2017). Although  $\alpha$ -tocopherol is poorly soluble in aqueous systems and very hard to integrate within film-forming, which are aqueous or hydrophilic systems, incorporation of  $\alpha$ -tocopherol in the biopolymer matrix is facilitated by emulsions or nanoemulsions (Pérez-Córdoba et al., 2018). For this reason, there is an opportunity to incorporate the active compounds of natural origin and recognized as GRAS into the packaging material (FDA, 2001), so that from the packaging, they exert their function as antioxidants and antifungals.

The primary objective was to evaluate the effect of the inclusion of natamycin, nanoemulsified  $\alpha$ -tocopherol, and a mixture of them on chemical, physical, mechanical properties, antioxidant, and antimicrobial activity of whey protein-based films.

## 2. Materials and methods

### 2.1. Raw materials and reagents

The following materials were used: Whey protein concentrate (WPC, 80% protein) obtained from Ingredientes y Productos Funcionales (IPF, Colombia), Natamycin (NAT), containing 50% lactose and 50% natamycin (ZSEB-E Co. Ltd, China),  $\alpha$ -tocopherol ( $\alpha$ -TOC) (97% Sigma-Aldrich), glycerol (Gly, J.T.Baker, Germany) used for film flexibility as a plasticizer, polysorbate 80 (Tween® 80, Sigma-Aldrich), sorbitan monoester (Span® 60, Sigma-Aldrich) as surfactants. Potassium persulfate, ABTS<sup>+</sup>: 2,2'-Azino-bis (3-ethylbenzenothiazoline-6-sulfonic acid), Trolox: 6-hydroxy-2,5,7,8-tetramethylchroman-2-carboxylic acid, chloride acid, ethanol, methanol, iron trichloride, acetate buffer, TPTZ: 2,4,6-Tri(2-pyridyl)-s-triazine and DPPH: 2,2-diphenyl-1-picrylhydrazyl of Sigma-Aldrich. The microorganisms used for testing were *C. albicans* ATCC 10231, *Saccharomyces cerevisiae* ATCC 2601, and *Penicillium chrysogenum* ATCC 10106 provided by Scorpionism Ofidism research group of University of Antioquia, the culture media used for fungi and yeasts were Sabouraud agar and Sabouraud broth (Merk, Germany).

### 2.2. Preparation of nanoemulsion of tocopherol

An oil-in-water (O/W) nanoemulsion was prepared at 1.29% (w/w)  $\alpha$ -TOC, by spontaneous emulsification followed by microfluidization, according to Bouchemal et al. (2004), Kaur et al. (2016), and Pérez-Córdoba et al. (2018), respectively. Two phases were prepared separately; an aqueous phase composed of 97.6% weight/weight (w/w) of distilled water and 0.30% (w/w) Tween 80 mixed at 25 °C/10 min with a magnetic stirrer (RH basic2, IKA, Germany); and an organic phase composed of 1.29% (w/w)  $\alpha$ -TOC, 0.19% (w/w) of Span 60 and 0.61% (w/w) of ethanol were mixed at 35 °C/10 min. Thereupon these phases were mixed and homogenized at 7000 rpm/5 min using an Ultra-Turrax (Ultra-Turrax® IKA T25, Labortechnik, Bodensee, Germany), achieving a hydrophilic-lipophilic balance (HLB = 11) to obtain a coarse emulsion. Finally, the nanoemulsion was obtained using a microfluidizer (M-110S, Microfluidics, USA) at 70 MPa and 3 processing cycles (Pérez-Córdoba et al., 2018).

### 2.3. Droplet size and stability of nanoemulsion of $\alpha$ -TOC

The stability and mean droplet size were measured using a multi-sample analytical centrifuge LUMiSizer® LS 610 (LUM GmbH, Berlin, Germany) at 20 °C and 865 nm. Nanoemulsion was centrifuged at 4000 rpm (2325.4  $\times$  g) for approximately 2 h (Dammak et al., 2017).

### 2.4. Films preparation

Four film-forming solutions (FFS) were formulated, as shown in Table 1. The FFS was prepared under continuous stirring dissolving WPC powder in distilled water, natamycin, nanoemulsified  $\alpha$ -TOC, or both and then glycerol added as a plasticizer, the pH of FFS was adjusted to 7 with 0.1 M NaOH (Ramos et al., 2013). Then, FFS was heated to 90 °C/20

min in a water bath (Marconi®, MA-184, SP, Brazil) and homogenized at 7000 rpm (Bonilla and Sobral., 2016).

Films were made by the solvent casting method in polystyrene Petri dishes (14 cm), dried at 30 °C/12 h in an oven (Marconis MA035/5, SP, Brazil). The films were conditioned in chambers carrying saturated solutions of NaBr (RH ≈ 58% and water activity,  $a_w \approx 0.575$ ) at 25 °C/7 days before all analyses. All characterizations were carried out in triplicates, at least.

## 2.5. Films characterization

### 2.5.1. Thickness

Film were measured using a digital micrometer (Mitutoyo IP65 Quantumike, Japan), at 10 random positions.

### 2.5.2. Moisture content

Moisture content (MC) (% w/w) was determined gravimetrically, following the methodology described by Ghadetaj et al. (2018), and Pérez-Córdoba et al. (2018).

### 2.5.3. Solubility in water

The solubility in water (S) (% w/w) was measured in discs of 20 mm diameter, which were weighed and shaken (60 rpm) with 50 mL of distilled water at 24 °C/24 h (Shaker SOLAB-SL223, Sao Paulo). The samples were removed from the distilled water and dried at 105 °C/24 h to know the final weight of dry matter (Pérez-Córdoba et al., 2018; Schmid et al., 2017).

### 2.5.4. Mechanical properties

The mechanical properties of films (ten samples sheets from each film) were measured determining EB: elongation at break, TS: tensile strength, and EM: elastic modulus by the ASTM D882/12 (ASTM, 2001) standard method using a texture analyzer (TA.XT2i, Stable Micro System, UK).

### 2.5.5. Optical properties (Color, opacity and UV-Vis light barrier)

The color values of films were determined using a colorimeter MiniScan MSEZ 1049 (HunterLab, Reston, VA, USA) with a measuring cell with an opening of 30 cm, D65 (daylight) lamp, angle of 10° (Bonilla and Sobral., 2016). The coordinates CIELab,  $L^*$  (lightness),  $a^*$  (red-green), and  $b^*$  (yellow-blue) were obtained, allowing the calculation of the total color difference ( $\Delta E^*$ ) using Eq. (1) (Dammak et al., 2017; Ghadetaj2018).

$$\Delta E^* = \sqrt{(\Delta L^*)^2 + (\Delta a^*)^2 + (\Delta b^*)^2} \quad (1)$$

Where

$$\Delta L^* = L^*_{sample} - L^*_{standard}$$

$$\Delta a^* = a^*_{sample} - a^*_{standard}$$

$$\Delta b^* = b^*_{sample} - b^*_{standard}$$

Moreover, film opacity was measured following the Hunterlab method in the reflectance mode, using the same equipment for the color analysis (Bonilla and Sobral., 2016).

The UV-Vis light barrier was measured as transmittance (%) using a UV-Vis spectrophotometer LAMBDA 35 (Perkin Elmer, Waltham, MA, USA) in wavelength range from 200 to 900 nm (Dammak et al., 2017; Ramos et al., 2012).

### 2.5.6. Water vapor permeability

Water vapor permeability (WVP) ( $\text{g}\cdot\text{m}^{-1}\cdot\text{s}^{-1}\cdot\text{Pa}^{-1}$ ) was obtained gravimetrically at 25 °C, according to the method reported by

Pérez-Córdoba et al. (2018). The aluminum cells had a permeation area of 0.0032  $\text{m}^2$ , and they contained silica gel (~0% RH). Films were disposed at the top of the cell and placed in a desiccator containing distilled water with 100% RH and were weighed for 7 days. The WVP was calculated as follow (Equation 2):

$$WVP = \left(\frac{w}{t}\right) \left(\frac{x}{A\Delta P}\right) \quad (2)$$

Where  $w/t$  ( $\text{g}\cdot\text{s}^{-1}$ ): coefficient of the linear regression,  $\Delta P$  (Pa): partial vapor pressure difference between water and the dry atmosphere (3169.1 Pa),  $x$  (mm): film thickness, and  $A$  ( $\text{m}^2$ ): permeation area. (Ahmed and Ikram., 2016; Bonilla and Sobral., 2016; Dammak et al., 2017; Marra et al., 2016) Three replicates per film were analyzed.

### 2.5.7. Microstructure: Scanning electron microscopy (SEM)

The microstructure of the cross-sections and the upper surface of the films samples were pre-conditioned using silica gel for 10 days at room temperature and were visualized by SEM, using a HITACHI Tabletop Microscope TM3000 (Hitachi Ltd, Tokyo, Japan), with a wide magnification range of 15–15,000X. The images were captured using an accelerating voltage of 15 kV.

### 2.5.8. Fourier-transform infrared spectroscopy (FTIR)

FTIR spectroscopy was used to analyze the chain interactions into films, the spectra of the films were obtained in transmittance mode from 650 to 4000  $\text{cm}^{-1}$  at a resolution of 1  $\text{cm}^{-1}$ , using a spectrometer (FTIR-ATR Spectrum One, Perkin Elmer) equipped with the Spectrum One software (Bonilla and Sobral., 2016; Lara et al., 2019).

### 2.5.9. Antioxidant properties

**2.5.9.1. Sample preparation.** The solutions containing  $\alpha$ -tocopherol were prepared by the extraction method described by Contreras-Calderón et al. (2011) with slight modifications; 0.1 g from each film were placed with 6 g of methanol-water (50:50, v/v), and were mixed in a vortex (BOECO, Germany) for 1 min, after that, the samples were shaken 1 h at 25 °C in a shaker (Heidolph Unimax 1010, Germany). The samples were centrifuged at 6000 rpm/10 min (BOECO C-28A, Germany), and the supernatant was recovery. The process was repeated but adding 6 g of acetone-water (60:40, v/v) to the residue, finally, it was adjusted up to 25 g with deionized water.

**2.5.9.2. ABTS<sup>•+</sup> method.** The ABTS free radical scavenging method was done according to previous works (Bonilla and Sobral., 2016; Contreras-Calderón et al., 2011; Dammak et al., 2017; López de Dicastillo et al., 2016; Pérez-Córdoba et al., 2018; Re et al., 1999). A solution of ABTS<sup>•+</sup> was prepared (1:1) with potassium persulfate (2.45 mM) and ABTS (7 mM), and kept for 16 h in the dark. Later, to prepare the ABTS<sup>•+</sup> working solution, an aliquot of ABTS<sup>•+</sup> solution was diluted with ethanol to reach an absorbance of  $0.70 \pm 0.02$ , using a UV-Vis spectrophotometer at 730 nm. Aqueous solutions of Trolox from 0 to 500  $\mu\text{M}$  were used for calibration. 100  $\mu\text{L}$  of film extraction, diluted with Trolox standard or water was added to 1 mL of ABTS<sup>•+</sup> working solution and hatched 30 min at 30 °C.

**2.5.9.3. DPPH<sup>•</sup> method.** Scavenging of DPPH<sup>•</sup> radical was measured using a modified Alam et al. (2013) method. 0.2 mL of film extraction and 2 mL of methanol was mixed, after that, 2 mL of DPPH<sup>•</sup> radical solution (120  $\mu\text{M}$ ) was added, and kept in the dark 30 min. Subsequently, the absorbance was determined at 515 nm using a UV-Vis spectrophotometer (Mapada-UV330 Shanghai, China).

**2.5.9.4. FRAP assay.** The FRAP assay was made following Contreras-Calderon et al. (2011). FRAP reagent was made with 2.5 mL of  $\text{FeCl}_3$  (20 mM), 25 mL acetate buffer 0.3 M at pH 3.6, and 2.5 mL of TPTZ

**Table 2.** Physicochemical and mechanical properties of WPC films incorporated with NAT or nanoemulsions of  $\alpha$ -TOC, or both. F0: Film without active compounds (Control film); F1: 2%  $\alpha$ -TOC – 0 ppm NAT; F2: 0%  $\alpha$ -TOC – 300 ppm NAT; F3: 2%  $\alpha$ -TOC – 300 ppm NAT.

Film	Thickness (mm)	Moisture content (%)	Solubility in water (%)	TS (MPa)	EB (%)	EM (MPa)
n	10	3	3	10	10	10
F0	0.122 ± 0.017 <sup>a</sup>	28.3 ± 2.3 <sup>a</sup>	58.9 ± 0.7 <sup>a</sup>	10.8 ± 0.6 <sup>a</sup>	29.4 ± 10.2 <sup>a</sup>	2.4 ± 0.4 <sup>a</sup>
F1	0.119 ± 0.037 <sup>a</sup>	28.3 ± 2.0 <sup>a</sup>	55.4 ± 1.1 <sup>b</sup>	3.3 ± 0.6 <sup>b</sup>	48.6 ± 14.9 <sup>b</sup>	0.8 ± 0.2 <sup>b</sup>
F2	0.124 ± 0.010 <sup>a</sup>	31.3 ± 5.7 <sup>b</sup>	58.8 ± 0.8 <sup>a</sup>	6.4 ± 0.9 <sup>c</sup>	45.6 ± 9.2 <sup>b</sup>	1.5 ± 0.3 <sup>c</sup>
F3	0.139 ± 0.020 <sup>a</sup>	29.5 ± 3.2 <sup>a</sup>	55.3 ± 1.5 <sup>b</sup>	5.9 ± 0.7 <sup>c</sup>	46.4 ± 11.5 <sup>b</sup>	1.3 ± 0.2 <sup>c</sup>

Mean values ± standard deviation. Different letters in the same column indicate significant differences ( $p < 0.05$ ) among the average values obtained by application of Duncan's test. TS: Tensile strength; EB: Elongation at break; EM: Elastic modulus.

(prepared in 40 mM HCl). After that, 30  $\mu$ L of film extract or Trolox was mixed with 90  $\mu$ L distilled water, 900  $\mu$ L of FRAP, and incubated at 35 °C/30 min. Absorbance values at 595 nm were measured using a UV-Vis spectrophotometer (Mapada-UV330 Shanghai, China), and for calibration curve was used solutions from 0 to 500  $\mu$ M of Trolox. The results for all antioxidant properties were expressed as Trolox Equivalent Antioxidant Capacity TEAC ( $\mu$ mol/g films).

### 2.5.10. Antimicrobial activity

**2.5.10.1. Growth conditions.** *Candida albicans* and *Saccharomyces cerevisiae* were grown in 100 mL Sabouraud broth at 37 °C/12 h in a continuously agitated shaker until its exponential growth phase. *Penicillium chrysogenum* was grown in inclined agar tubes using 50 mL Sabouraud agar at 37 °C until sporulation was reached. On the day of the antimicrobial test, the spores were scraped off with sterile water (Ciro2014; Ollé Resa, Gerschenson and Jagus., 2014a).

**2.5.10.2. Agar diffusion method.** The antimicrobial effect of films on the test microorganisms was evaluated by the agar diffusion method. 100  $\mu$ L of inoculum with turbidity equivalent to a McFarland 0.5 (using a spectrophotometer at 625nm) containing  $1.5 \times 10^8$  CFU/mL of each microorganism, *C. albicans*, *S. cerevisiae*, and *P. chrysogenum* were prepared and spread on the surface of Petri dishes carrying Sabouraud agar (Bonilla and Sobral., 2016; Ciro2014).

Discs of 7 mm diameter were cut from treatments F0 (negative control), F2, F3 and positive control (discs from filter paper soaked with 300 ppm NAT) were placed on each plate previously inoculated, after that all plates are incubated at 25 °C/24 h (Ollé Resa, Gerschenson and Jagus., 2014a). The zone of inhibition ( $\text{mm}^2$ ) was calculated from the area of the whole zone subtracted from the disc area.

### 2.5.11. Statistical analysis

Statistical analyses of data were performed through a variance analysis (ANOVA) employment the Statgraphics® centurion XV software. The differences were tested using Duncan's multiple range test at  $p < 0.05$ .

## 3. Results and discussion

### 3.1. Characterization of nanoemulsion

It is necessary to ensure the quality of the nanoemulsion of  $\alpha$ -TOC production before applying it to WPC film to guarantee that it will be stable during film processing. In this sense, the evaluation of the mean droplet size and nanoemulsion stability is indispensable. Then, the nanoemulsion presented a monomodal distribution, with an average diameter of  $113.50 \pm 1.6$  nm. Pérez-Córdoba et al. (2018) reported similar results about the mean droplet size for nanoemulsions of  $\alpha$ -tocopherol/cinnamaldehyde, and  $\alpha$ -tocopherol/garlic oil,  $123.1 \pm 1.5$  nm,  $111.0 \pm 2.0$  nm respectively. The experimental results of the stability showed that stability values for nanoemulsion correspond to 0.588 for

the first month, and 0.481 a second month. Values less than 0.5 indicate a phase separation and instability of nanoemulsions (Dammak2019).

### 3.2. Film characterization

All WPC films were transparent, with no apparent defects by naked eye observation such as bubbles, scratches, phase separation, or cracks. The thickness was maintained in all films (Table 2), and no statistical difference was observed between data ( $p = 0.30$ ), allowing to calculate an average thickness of  $0.126 \pm 0.021$  mm, comparable to those reported by Ramos et al. (2013) with a thickness of  $0.13 \pm 0.04$  mm for films produced with film-forming solution with the same protein concentration. Therefore, the addition of active compounds did not modify this property.

#### 3.2.1. Moisture content (MC) and solubility (S) in water

Table 2 presented the values obtained for S and MC for WPC films. No significant difference ( $p = 0.72$ ) was observed for MC of all films, allowing calculation of an average value of 28.6 g of water/100 g of dry matter. Neither NAT, nanoemulsion of  $\alpha$ -TOC, or both did not modify the hygroscopicity, as Pérez-Córdoba et al. (2018) showed in chitosan-gelatin films. These results are interesting because eventual differences in MC could affect the results of some physical properties owing to the plasticizing effect of water.

Regarding film solubility in water, it was observed that F1 and F3 showed slightly lower S ( $p < 0.05$ ) than the F0 and F2, whereas no significant difference ( $p > 0.05$ ) was observed between these last two films. According to these results, the presence of the nanoemulsified  $\alpha$ -TOC contributed to reducing the solubility of the film, and all results of S showed that WPC films maintain their integrity after 24 h in water, due to the establishment of disulfide bonds between protein molecules generated after the heat treatment (Ramos et al., 2013).

#### 3.2.2. Mechanical properties

The incorporation of active compounds produced films (F1, F2, F3) with lower TS and EM, which means, less resistant and stiff films, and higher EB, or more stretchable one, than F0 ( $p < 0.05$ ) (Table 2). Nevertheless, NAT was the active component that provoked the less considerable changes in TS and EM of films (F2, F3). Thus, the film (F1) with only nanoemulsified  $\alpha$ -tocopherol presented the lower values of TS ( $p < 0.05$ ) and EM. Interestingly, this behavior was not observed for EB, where all films (F1, F2, F3) presented similar values ( $p > 0.05$ ). Apparently, the active compounds seem to present a plasticizer effect on films.

TS values significantly decreased from  $10.8 \pm 0.6$  (F0) to  $3.3 \pm 0.6$  MPa (F1) ( $p < 0.05$ ) for films loaded with nanoemulsified  $\alpha$ -tocopherol (Table 2). These results of weaker films agree with those presented by Ramos et al. (2012) with antimicrobial agents including natamycin on WPI films, alginate/pectin films loaded with NAT Krause et al. (2012) and Noronha et al. (2014) on methylcellulose films loaded with  $\alpha$ -tocopherol nanocapsules. Also, Martins et al. (2012) found on chitosan films that  $\alpha$ -tocopherol incorporation reduced TS ( $p < 0.05$ ), and Bahram

**Table 3.** Color ( $L^*$ : Luminosity,  $a^*$ : Chroma range green-red,  $b^*$ : Chroma range blue-yellow,  $\Delta E^*$ : total color difference), opacity, and water vapor permeability of WPC films. F0: Film without active compounds (Control film); F1: 2%  $\alpha$ -TOC – 0 ppm NAT; F2: 0%  $\alpha$ -TOC – 300 ppm NAT; F3: 2%  $\alpha$ -TOC – 300 ppm NAT.

Film	$L^*$	$a^*$	$b^*$	$\Delta E^*$	Opacity	WVP ( $\times 10^{-10} \text{ g.m}^{-1} \text{ s}^{-1} \text{ Pa}^{-1}$ )
F0	89.7 $\pm$ 0.4 <sup>a</sup>	-1.9 $\pm$ 0.1 <sup>a</sup>	9.8 $\pm$ 1.3 <sup>a</sup>	9.0 $\pm$ 1.4 <sup>a</sup>	4.2 $\pm$ 0.6 <sup>a</sup>	1.4 $\pm$ 0.0 <sup>a</sup>
F1	90.9 $\pm$ 0.6 <sup>b</sup>	-1.5 $\pm$ 0.1 <sup>b</sup>	10.7 $\pm$ 1.6 <sup>b,c</sup>	9.5 $\pm$ 1.7 <sup>a,b</sup>	5.9 $\pm$ 0.7 <sup>b</sup>	1.9 $\pm$ 0.1 <sup>b</sup>
F2	90.5 $\pm$ 0.3 <sup>c</sup>	-1.3 $\pm$ 0.1 <sup>c</sup>	10.2 $\pm$ 0.8 <sup>a,b</sup>	9.1 $\pm$ 0.8 <sup>a</sup>	6.5 $\pm$ 1.0 <sup>c</sup>	1.3 $\pm$ 0.1 <sup>c</sup>
F3	90.9 $\pm$ 0.3 <sup>b</sup>	-1.6 $\pm$ 0.1 <sup>d</sup>	11.4 $\pm$ 0.9 <sup>c</sup>	10.0 $\pm$ 0.9 <sup>b</sup>	6.1 $\pm$ 0.5 <sup>b,c</sup>	1.6 $\pm$ 0.0 <sup>d</sup>

Mean values  $\pm$  standard deviation,  $n = 3$ . Different letters in the same column indicate significant differences ( $p < 0.05$ ) among the average values obtained by application of Duncans test.

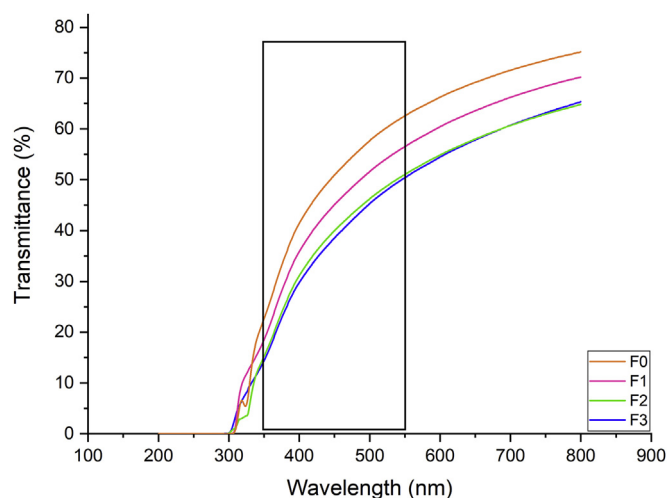


**Figure 1.** Light transmission spectra (UV-Vis) of WPC film loaded with nanoemulsified  $\alpha$ -TOC, NAT, and its mixture. F0: Film without active compounds (Control film); F1: 2%  $\alpha$ -TOC – 0 ppm NAT; F2: 0%  $\alpha$ -TOC – 300 ppm NAT; F3: 2%  $\alpha$ -TOC – 300 ppm NAT.

et al. (2014) noted that the presence of Cinnamon Essential Oil inside to WPC films caused a decrease in TS ( $p < 0.05$ ). Pérez-Córdoba et al. (2018) also have similar behavior for TS on gelatin-chitosan films incorporated with  $\alpha$ -tocopherol, garlic oil, and cinnamaldehyde. The addition of  $\alpha$ -TOC inside WPC film produces a film structure with less chain mobility, flexibility, and resistance to fracture Martins et al. (2012).

The EM results behave like those of TS. The addition of nanoemulsion of  $\alpha$ -TOC, NAT, or both into the WPC-films reduced the stiffness ( $p < 0.05$ ) because these compounds modified the intermolecular linkage in the protein chains (Ghadetaj et al., 2018). In general, a high EM could be expected since a higher degree of denaturation generates more disulfide bonds. Nevertheless, the addition of nanoemulsions of  $\alpha$ -TOC with hydrophobic ingredients and surfactants modified their interactions with film materials. Furthermore, it might perform a plasticizer action and increase polymer mobility.

Analogous effects have been shown on WPI films with the addition of *Grammosciadium ptrocarpum* Bioss essential oils (Ghadetaj et al., 2018) and Natamycin (Ramos et al., 2012). The EB in control (F0) film was 29.4% (Table 2), the inclusion of nanoemulsified  $\alpha$ -TOC, NAT, or both (F1, F2, and F3) did not change EB significantly between these last ones ( $p > 0.05$ ). Bahram et al. (2014) revealed a growth in EB by the addition of cinnamon essential oil or lipids in protein films. The films loaded of compounds are higher than the control; these results reflect the grade of chemical and structural compatibility of compounds on WPC films.

### 3.2.3. Optical properties (Color, opacity and UV-Vis light barrier)

Color measurements to WPC films are shown in Table 3. These attributes can affect product appearance and consumer acceptability.

According to these results (Table 3), compounds loaded led to an increase in the  $L^*$ ,  $a^*$ ,  $b^*$ , and opacity values of the produced films.

Although  $L^*$  and  $a^*$  show some significant difference ( $p < 0.05$ ), this value was around 90 and -1.5; hence these films presented a slightly yellowish color and translucent. These values were higher than WPI films with nanoemulsions of *Grammosciadium ptrocarpum* Bioss this value the  $L^*$ ,  $a^*$  was 82 and -5.5, respectively (Ghadetaj et al., 2018). Also, Ghadetaj et al. (2018) showed that the incorporation of nanoemulsions had no significant effect on the  $L^*$ ,  $a^*$ , and  $b^*$  values of WPI films. Regarding the results of  $\Delta E^*$ , it was observed that WPC-film had a yellow aspect, and the  $\Delta E^*$  value of the control film (F0) was  $9.0 \pm 1.4$  (Table 3). The addition of additives increased  $\Delta E^*$  value ( $p < 0.05$ ), with the highest  $\Delta E^*$  ( $10.0 \pm 0.9$ ) observed for F3, as a consequence of the yellow color of  $\alpha$ -TOC. This result was consistent with Bahram et al. (2014), which found that the incorporation of Cinnamon Essential Oil into WPC films increases the  $\Delta E^*$  value of WPC film.

The films were virtually transparent (opacity  $\sim 0$ ). Films were less transparent when the active compounds are added in its structure (F1, F2, and F3) presenting values of 5.9, 6.5, and 6.1, respectively (Table 3). The films presented a rise in opacity caused by natamycin, and this may be associated to the low solubility of natamycin in water whose substance was 50% pure in lactose; also, the natamycin molecule has a hydrophobic and hydrophilic component Krause et al. (2012). Also, it can be affected by the procedure steps, the size, and concentration of the loaded compounds.

The light transmission of all films is shown in Figure 1. All WPC films have high barrier properties in the UV range (200–300 nm), which may be due to the high content of aromatic amino acids in the proteins into films, that can absorb UV (Ramos et al., 2012), independently of the presence of the active components. Regarding the visible light, the domain comprising wavelengths of 350–550 nm are the most damaging (rectangle in Figure 1), the maximum damage occurring at about 450 nm (Robertson., 2013), provoking chemical reactions induced by visible light (e.g., Vitamin B2). Then, in this domain, the F3 and F2 presented the best barrier to light (Figure 1).

### 3.2.4. Water vapor permeability (WVP)

WVP is an important property for biodegradable films since it is essential to determine the feasibility of films to avoid deterioration reactions in foods (Martins et al., 2012).

The presence of nanoemulsified  $\alpha$ -TOC, NAT, or both changed WVP values in films and their values are presented in Table 3. Despite of the significant differences between all films, the values are very close, and with the same order of magnitude. The F0 film showed a value for WVP of  $1.4 \times 10^{-10} \text{ g.m}^{-1} \text{ s}^{-1} \text{ Pa}^{-1}$  and it increases to  $1.9 \times 10^{-10} \text{ g.m}^{-1} \text{ s}^{-1} \text{ Pa}^{-1}$  (F1) and  $1.6 \times 10^{-10} \text{ g.m}^{-1} \text{ s}^{-1} \text{ Pa}^{-1}$  (F3) (Table 3). Although  $\alpha$ -TOC is hydrophobic, WVP values increased when nanoemulsified  $\alpha$ -TOC was incorporated into WPC films. Maybe the effect of nanoemulsified  $\alpha$ -TOC over the cohesion forces of the protein network lets the movement of water vapor throughout the WPC matrix (Ghadetaj et al., 2018; Ramos et al., 2013) and in chitosan-based films containing  $\alpha$ -tocopherol (Martins et al., 2012). Besides, nanoemulsified  $\alpha$ -TOC incorporated increases the molecular spaces between the protein

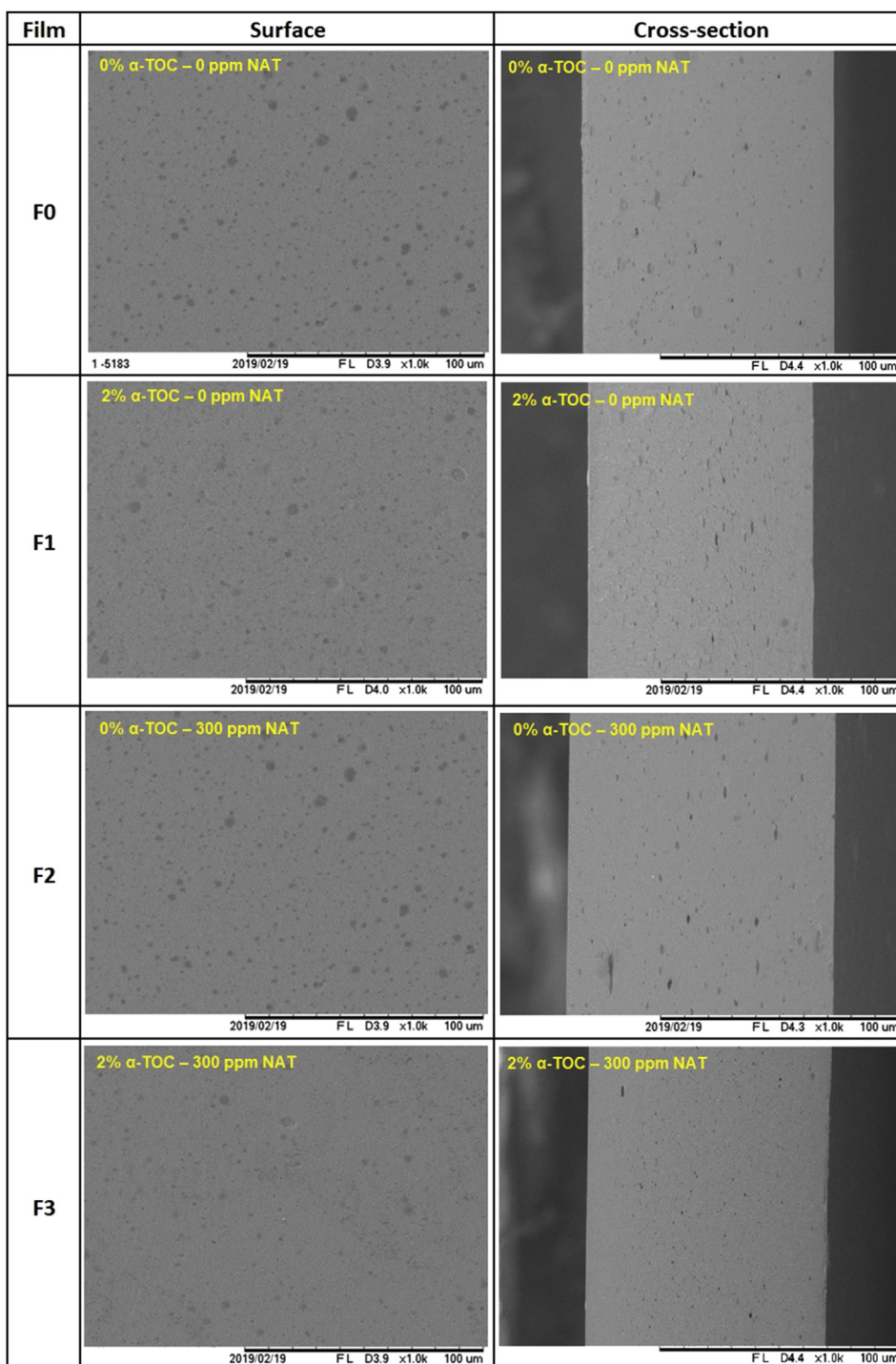


**Figure 2.** SEM micrographs of the surface and cross-section of whey protein concentrate films incorporated with nanoemulsified  $\alpha$ -TOC, NAT, and its mixture. F0: Film without active compounds (Control film); F1: 2%  $\alpha$ -TOC – 0 ppm NAT; F2: 0%  $\alpha$ -TOC – 300 ppm NAT; F3: 2%  $\alpha$ -TOC – 300 ppm NAT.

network and reduces the intermolecular interaction which is why increasing the permeability of WPC films.

However, natamycin exhibited a decrease of WVP with a value of  $1.3 \times 10^{-10} \text{ g.m}^{-1}.\text{s}^{-1}.\text{Pa}^{-1}$  (F2) and this value are much lower than the control film, whose value was  $1.4 \times 10^{-10} \text{ g.m}^{-1}.\text{s}^{-1}.\text{Pa}^{-1}$ . Ramos et al. (2012) and Ollé Resa et al. (2014b) noted a similar result with a significant difference for tapioca starch films in which the use the natamycin reduced the WVP value. Thus, all films, independently of additives, were high permeable to the water vapor.

### 3.2.5. Microstructure

Figure 2 shows SEM micrographs of cross-sections and surface morphology. Surfaces with some heterogeneous surface can be observed in all films, with circular structures seems having be occupied by glycerol droplets, distributed in the cross-section. On another side, eventually separation between the active compounds and the WPC was not observed, indicating a high compatibility of the nanoemulsified  $\alpha$ -TOC, NAT and its mixture with the film matrix, producing a relatively smooth and compact morphology. Moreover, some open porous was observed in the cryo-fractured surface of films (Figure 2). Similar results were

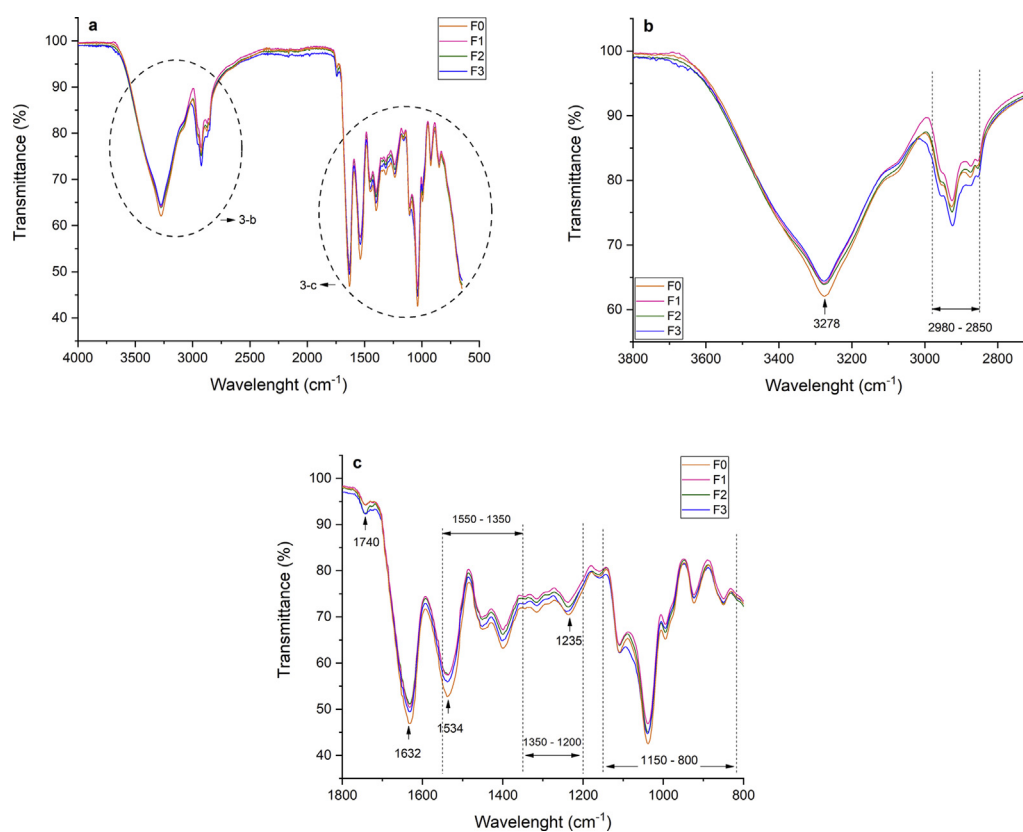


**Figure 3.** FT-IR spectra of WPC film loaded with O/W nanoemulsions  $\alpha$ -TOC, NAT, and its mixture: (a) range at 4000 - 600  $\text{cm}^{-1}$ ; (b) range at 3800 - 2700  $\text{cm}^{-1}$  and (c) range at 800 - 1800  $\text{cm}^{-1}$ . F0: Film without active compounds (Control film); F1: 2%  $\alpha$ -TOC - 0 ppm NAT; F2: 0%  $\alpha$ -TOC - 300 ppm NAT; F3: 2%  $\alpha$ -TOC - 300 ppm NAT.

obtained by Noronha et al. (2014) using  $\alpha$ -TOC nanocapsules loaded in methylcellulose film, which observed a smooth and compact structure probably due to the strong chemical bond of each component loaded.

The incorporation of nanoemulsion can decrease the miscibility of WPC-films, whereas producing a less compact and more porous structure (Oymaci and Altinkaya, 2016). The little orifices in all films were the marks of droplets that remained in the film during fracturing with nitrogen. Film F2 showed a surface free of crystals, in comparison to those presented by Krause et al. (2012) with alginate/pectin films that indicate that the added of natamycin showed the presence of crystals and a surface with non-uniform.

### 3.2.6. Fourier-transform infrared spectroscopy

FTIR spectroscopy was used to determine  $\alpha$ -TOC and NAT presence and know structural changes on WPC films (Figure 3). All WPC films spectra showed bands ranging from 3150 to 3600  $\text{cm}^{-1}$  attributed to free OH and N-H groups on protein strands, respectively; the bands from 2850 to 2980  $\text{cm}^{-1}$  associated to C-H stretching bond, the peaks from

1600 to 1700  $\text{cm}^{-1}$  are attributed to Amide-I related to C=O stretch and C-N vibrations; the peaks from 1400 to 1550  $\text{cm}^{-1}$  assigned to Amide-II (groups N-H); the peaks on 1200-1350  $\text{cm}^{-1}$  related to Amide III with C-N stretching and N-H bonds, peaks from 800 to 1150  $\text{cm}^{-1}$  associated to absorption bonds of glycerol (Ghadetaj et al., 2018; Ramos et al., 2013).

By the addition of NAT (F2), the peak value increase in the range of 2920  $\text{cm}^{-1}$  associated with C-H stretching vibration, it is also represented in the F3 film. The peaks ranging from 3500  $\text{cm}^{-1}$  to 3350  $\text{cm}^{-1}$  are also characteristic of N-H stretch of natamycin and possibly were overlaid by O-H peaks of Gly,  $\alpha$ -TOC, and WPC; similar changes are shown in alginate active films with natamycin (Bierhalz et al., 2013) and polyethylene with natamycin (Grafia et al., 2018). For F1, the intensity of the band in 2920  $\text{cm}^{-1}$  decreased, Martins et al. (2012) showed the possibly the creation of new connections on film by the presence of  $\alpha$ -TOC and surfactant. For F3, the band intensity in 3278  $\text{cm}^{-1}$  decreased, which is associated to N-H free O-H protein.

**Table 4.** Trolox Equivalent Antioxidant Capacity (TEAC) and Inhibition halos against *Candida albicans*, *Penicillium chrysogenum* and *Saccharomyces cerevisiae* of WPC films. F0: Film without active compounds (Control film); F1: 2%  $\alpha$ -TOC - 0 ppm NAT; F2: 0%  $\alpha$ -TOC - 300 ppm NAT; F3: 2%  $\alpha$ -TOC - 300 ppm NAT.

Film	TEAC ( $\mu\text{mol TE/g}$ dried film)			Zone of inhibition ( $\text{mm}^2$ )		
	ABTS* <sup>+</sup>	FRAP	DPPH*	<i>C. albicans</i>	<i>P. chrysogenum</i>	<i>S. cerevisiae</i>
F0	0.0 $\pm$ 0.0 <sup>a</sup>	0.0 $\pm$ 0.0 <sup>a</sup>	0.0 $\pm$ 0.0 <sup>a</sup>	0.0 $\pm$ 0.0 <sup>a</sup>	0.0 $\pm$ 0.0 <sup>a</sup>	0.0 $\pm$ 0.0 <sup>a</sup>
F1	19.5 $\pm$ 1.1 <sup>b</sup>	9.5 $\pm$ 0.9 <sup>b</sup>	28.8 $\pm$ 0.5 <sup>b</sup>	-	-	-
F2	0.0 $\pm$ 0.0 <sup>a</sup>	0.0 $\pm$ 0.0 <sup>a</sup>	0.0 $\pm$ 0.0 <sup>a</sup>	170.1 $\pm$ 22.0 <sup>b</sup>	315.3 $\pm$ 35.5 <sup>b</sup>	334.9 $\pm$ 40.5 <sup>b</sup>
F3	14.6 $\pm$ 1.2 <sup>c</sup>	4.4 $\pm$ 1.0 <sup>c</sup>	26.5 $\pm$ 0.7 <sup>c</sup>	150.9 $\pm$ 29.3 <sup>b</sup>	288.2 $\pm$ 39.6 <sup>b</sup>	303.5 $\pm$ 14.5 <sup>b</sup>

Mean values  $\pm$  standard deviation. Different letters in the same column indicate significant differences ( $p < 0.05$ ) among the average values obtained by application of Duncan's test.

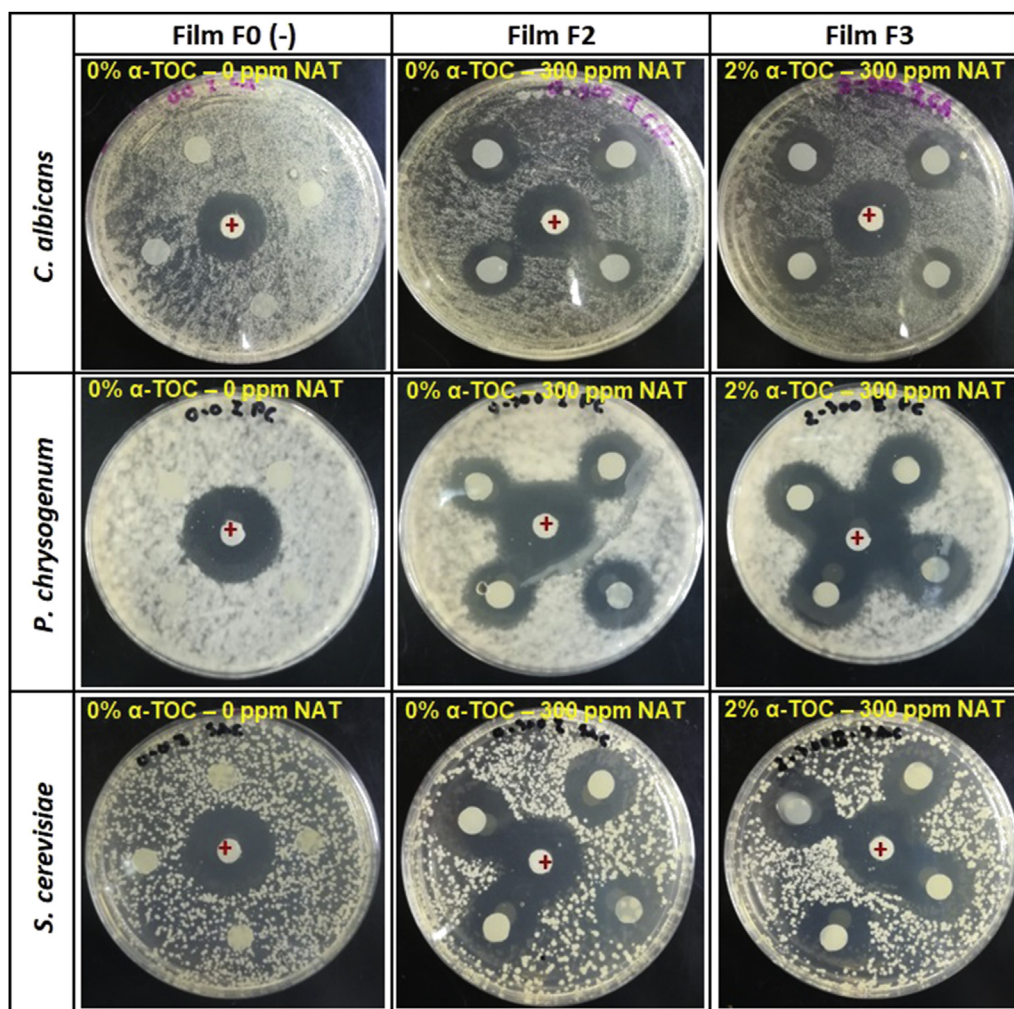


**Figure 4.** Inhibition of *Candida albicans*, *Penicillium chrysogenum* and *Saccharomyces cerevisiae* following disk diffusion assay of WPC films. F0: Film without active compounds (Control film); F1: 2%  $\alpha$ -TOC – 0 ppm NAT; F2: 0%  $\alpha$ -TOC – 300 ppm NAT; F3: 2%  $\alpha$ -TOC – 300 ppm NAT.

Generally, active compounds were stayed in the network of the WPC film by the establishment of chemical bonds and by physical entrapment too. Bahram et al. (2014) with adding cinnamon essential oil and Ghadetaj et al. (2018) with the inclusion of *Grammosciadium ptoecarpum* Bioss essential oils have shown similar results on the structural properties of the films.

### 3.2.7. Antioxidant activity

The antioxidant activity of the WPC films, determined by ABTS<sup>•+</sup>, DPPH<sup>•</sup>, and FRAP, and was expressed as  $\mu\text{mol TE/g}$  film, and are presented in Table 4. As predictable, F0 and F2 did not present any radical scavenging activity in tested methods because neither WPC nor NAT have this property. Only films containing  $\alpha$ -TOC (F1 and F3) showed antioxidant activity. The  $\alpha$ -TOC can donate a hydrogen atom to quench free radicals by producing  $\alpha$ -tocopheroxyl radicals until the decolorization of ABTS and DPPH radical, respectively (Re et al., 1999; Contreras-Calderón et al., 2011).

The film F1 presented an antioxidant activity higher ( $p < 0.05$ ) than F3, suggesting that NAT reduced the action of  $\alpha$ -TOC, or, in other words, they have antagonist effect. F1 presented an antioxidant activity of  $19.5 \pm 1.1$ ,  $9.5 \pm 0.9$ , and  $28.8 \pm 0.5$   $\mu\text{mol TE/g}$  film for ABTS<sup>•+</sup>, FRAP and DPPH<sup>•</sup>, respectively. F3 presented values of  $14.6 \pm 1.2$ ,  $4.4 \pm 1.0$ , and  $26.5 \pm 0.7$   $\mu\text{mol TE/g}$  film in the same order (Table 4). Although F3 has natamycin together with  $\alpha$ -TOC its antioxidant capacity (ABTS<sup>•+</sup> and DPPH<sup>•</sup>) is even higher than shown in gelatin films loaded with

$\alpha$ -tocopherol which published values of  $2.6 \pm 0.1$  and  $0.2 \pm 0.0$   $\mu\text{mol TE/g}$  film for ABTS<sup>•+</sup> and DPPH<sup>•</sup> respectively (Pérez et al., 2018).

### 3.2.8. Antimicrobial activity

As a could be expected, the WPC films with natamycin (F2 and F3) were efficacious against *C. albicans*, *P. chrysogenum*, and *S. cerevisiae* when evaluated an agar diffusion method (Figure 4, Table 4). Among additives, only natamycin has antimicrobial activity. Thus, films F0 and F1 (without natamycin) did not show antimicrobial activity, whereas films F2 and F3 presented an area of inhibition more extensive than control films, owing to the diffusion of antimicrobial across the WPC films, and the presence of  $\alpha$ -TOC (F3) only leads to a reduction in inhibition area nevertheless did not modify the antimicrobial activity of the films ( $p > 0.05$ ). Ollé Resa et al. (2014b) published analogous results about the antimicrobial activity against *S. cerevisiae* on starch edible films, Ramos et al. (2012) reported that whey protein isolate films loaded with natamycin present inhibition against one yeast, *Y. lipolytica*. Also, Fajardo et al. (2010) evaluated that chitosan coating loaded with natamycin against *Penicillium crustosum*, *P. roqueforti*, *P. commune*, and *Aspergillus niger*. These studies showed that natamycin obstacle fungal growth by attachment particularly to ergosterol, which is only present in moulds and yeast plasma membranes. The natamycin impedes vacuolar by interaction with ergosterol (Ollé Resa, Gerschenson, and Jagus., 2014a). The diffusion of NAT into agar gel was similar for the yeast and moulds test due to the same agar was used for their growth, nevertheless the different diameters obtained were related with sensitivity to

natamycin and different growth rate for the microorganisms tested (Figure 4 and Table 4).

#### 4. Conclusion

WPC films loaded with  $\alpha$ -tocopherol and natamycin were successfully prepared by the casting method. The characterization of the WPC films showed that active compounds are well distributed. The incorporation of  $\alpha$ -tocopherol and natamycin into WPC film did not affect the moisture content, nevertheless decreased the TS, EM and increased EB, showing that the nanoemulsified  $\alpha$ -TOC had a plasticizer effect on films. Water vapor permeability of the film increased despite the hydrophobic nature of  $\alpha$ -tocopherol but not increased for film with NAT. All films have an excellent barrier property in the UV region (200–550 nm). The FTIR spectra indicated that nanoemulsified  $\alpha$ -tocopherol, and natamycin remained stable during the process of making the films, which shown antioxidant capacity and antimicrobial activity against *C. albicans*, *P. chrysogenum*, and *S. cerevisiae* respectively.

The WPC films added with nanoemulsified  $\alpha$ -TOC, and natamycin have great potential for application in food packaging as a vehicle for active compounds and becoming as an alternative to typical materials for possibly enhancing safety, improving quality and increasing the shelf life of food packaged with them.

#### Practical applications

This research develops a food active packaging from renewable sources such as whey protein, with nanoemulsified  $\alpha$ -tocopherol and natamycin as antioxidant and antimicrobial compounds for better food protection. Physicochemical, mechanical, optical-properties, water vapor barrier, FTIR microstructure, antioxidant and antimicrobial activity were characterized to evaluate the potential for practical application as active packaging for the food industry.

#### Declarations

##### Author contribution statement

Camilo Agudelo-Cuartas: Conceived and designed the experiments; Performed the experiments; Analyzed and interpreted the data; Contributed reagents, materials, analysis tools or data; Wrote the paper.

Diana Granda-Restrepo: Conceived and designed the experiments; Analyzed and interpreted the data; Contributed reagents, materials, analysis tools or data; Wrote the paper.

Paulo J.A. Sobral: Analyzed and interpreted the data; Contributed reagents, materials, analysis tools or data; Wrote the paper.

Hugo Hernandez, Wilson Castro: Analyzed and interpreted the data; Wrote the paper.

##### Funding statement

Camilo Agudelo Cuartas was supported by the Fondo Nacional de Financiamiento para la Ciencia, la Tecnología y la Innovación "Francisco José de Caldas" a Colombian doctoral scholarship COLCIENCIAS (Convocatoria 727 of 2015).

##### Competing interest statement

The authors declare no conflict of interest.

##### Additional information

No additional information is available for this paper.

#### Acknowledgements

Agudelo Cuartas gratefully acknowledge Laboratorio de Tecnología de Alimentos (Universidad de Sao Paulo, Brasil), Universidad Nacional de Frontera, Sullana - Perú, Proyecto: Creación del Laboratorio de Investigación en Inocuidad (CUI N° 2439545), and Ingredientes y Productos Funcionales (IPF, Colombia).

#### References

- Ahmed, S., Ikram, S., 2016. Chitosan and gelatin based biodegradable packaging films with UV-light protection. *J. Photochem. Photobiol. B Biol.* 163, 115–124.
- Alam, Md. Nur., Jahan, N., Rafiquzzaman, Md., 2013. Review on in vivo and in vitro methods evaluation of antioxidant activity. *Saudi Pharmaceut. J.* 21 (2), 143–152.
- Altenhofen, M., Krause, A., Kieckbusch, T., 2012. Modelling natamycin release from alginate/chitosan active films. *Int. J. Food Sci. Technol.* 47 (4), 740–746.
- ASTM, 2001. Standard test method for tensile properties of thin plastic sheeting. *Standards Designations: D882. Annual Book of ASTM Standards.* American Society for Testing and Materials, Philadelphia, PA, USA, pp. 162–170.
- Atares, L., Chiralt, A., 2016. Essential oils as additives in biodegradable films and coatings for active food packaging. *Trends Food Sci. Technol.* 48, 51–62.
- Bahram, S., Rezaei, M., Soltani, M., Kamali, A., et al., 2014. Whey protein concentrate edible film activated with cinnamon essential oil. *J. Food Process. Preserv.* 38 (3), 1251–1258.
- Bierhalz, A., Sa Silva, M., de Sousa, H., Braga, M., et al., 2013. Influence of natamycin loading methods on the physical characteristics of alginate active films. *J. Supercrit. Fluids* 76, 74–82.
- Bonilla, J., Sobral, P.J.A., 2016. Investigation of the physicochemical, antimicrobial and antioxidant properties of gelatin-chitosan edible film mixed with plant ethanolic extracts. *Food Biosci.* 16, 17–25.
- Bouchemal, K., Briançon, S., Perrier, E., Fessi, H., 2004. Nano-emulsion formulation using spontaneous emulsification: solvent, oil and surfactant optimisation. *Int. J. Pharm.* 280 (1–2), 241–251.
- Cazón, P., Velázquez, G., Ramírez, J., Vázquez, M., 2017. Polysaccharide-based films and coatings for food packaging: a review. *Food Hydrocolloids* 68, 136–148.
- Ciro, G., Zapata, J.E., López, J., 2014. In vitro evaluation of bixa orellana L. (Annatto) seeds as potential natural food preservative. *J. Med. Plants Res.* 8 (21), 772–779.
- Contreras-Calderón, J., Calderón-Jaimes, L., Guerra-Hernández, E., García-Villanova, B., 2011. Antioxidant capacity, phenolic content and Vitamin C in pulp, peel and seed from 24 exotic fruits from Colombia. *Food Res. Int.* 44 (7), 2047–2053.
- Dammak, I., de Carvalho, R., Fávoro, C., Laureço, R., et al., 2017. Properties of active gelatin films incorporated with rutin-loaded nanoemulsions. *Int. J. Biol. Macromol.* 98, 39–49.
- Dammak, I., Lourenço, R., Sobral, P.J.A., 2019. Active gelatin films incorporated with pickering emulsions encapsulating hesperidin: preparation and physicochemical characterization. *J. Food Eng.* 240, 9–20.
- Fajardo, P., Martins, J.T., Fuciños, C., Pastrana, et al., 2010. Evaluation of a chitosan-based edible film as carrier of natamycin to improve the storability of saloio cheese. *J. Food Eng.* 101 (4), 349–356.
- FDA, 2001. CFR - Code of federal Regulations title 21. Part 182 substances generally recognized as safe. *Food Drug Admin.*
- Ghadetaj, A., Almasi, H., Mehryar, L., 2018. Development and characterization of whey protein isolate active films containing nanoemulsions of Grammoscadium procarpum Bioss. Essential oil. *Food Packag. Shelf Life* 16, 31–40.
- Grafia, A., Vázquez, M., Bianchinotti, M., Barbosa, S., 2018. Development of an antifungal film by polyethylene surface modification with natamycin. *Food Packag. Shelf Life* 18, 191–200.
- Granda-Restrepo, D., Soto-Valdez, H., Peralta, E., Troncoso-Rojas, R., et al., 2009. Migration of  $\alpha$ -tocopherol from an active multilayer film into whole milk powder. *Food Res. Int.* 42 (10), 1396–1402.
- Kaur, K., Kaur, J., Kumar, R., Mehta, S.K., 2016. Formulation and physicochemical study of A-tocopherol based oil in water nanoemulsion stabilized with non toxic, biodegradable surfactant: sodium stearoyl lactate. *Ultrasonics Sonochem.*
- Khalil, H.P.S., Davoudpour, Y., Saurabh, C., Hossain, M.D., et al., 2016. A review on nanocellulosic fibres as new material for sustainable packaging: process and applications. *Renew. Sustain. Energy Rev.* 64, 823–836.
- Krause, A., Altenhofen, M., Kieckbusch, T., 2012. Natamycin release from alginate/pectin films for food packaging applications. *J. Food Eng.* 110 (1), 18–25.
- Lara, B., Araújo, A., Dias, M., Guimarães, M., et al., 2019. Morphological, mechanical and physical properties of new whey protein isolate/polyvinyl alcohol blends for food flexible packaging. *Food Packag. Shelf Life* 19, 16–23.
- Lavoine, N., Guillard, V., Desloges, I., Gontard, N., Bras, J., 2016. Active bio-based food-packaging: diffusion and release of active substances through and from cellulose nanofiber coating toward food-packaging design. *Carbohydr. Polym.* 149, 40–50.
- López de Dicastillo, C., Rodríguez, F., Guarda, A., Galotto, M.J., 2016. Antioxidant films based on cross-linked methyl cellulose and native Chilean berry for food packaging applications. *Carbohydr. Polym.* 136, 1052–1060.
- Marra, A., Silvestre, C., Duraccio, C., Cimmino, S., 2016. Polylactic acid/zinc oxide biocomposite films for food packaging application. *Int. J. Biol. Macromol.* 88, 254–262.
- Martelli, S., Motta, C., Caon, T., Alberton, J., et al., 2017. Edible carboxymethyl cellulose films containing natural antioxidant and surfactants:  $\alpha$ -Tocopherol stability, in vitro release and film properties. *LWT-Food Sci. Technol.* 77, 21–29.

- Martins, J., Cerqueira, M., Vicente, A., 2012. Influence of  $\alpha$ -tocopherol on physicochemical properties of chitosan-based films. *Food Hydrocolloids* 27 (1), 220–227.
- Moatsou, G., Moschopoulou, E., Beka, A., Tsermoula, P., 2015. Effect of natamycin-containing coating on the evolution of biochemical and microbiological parameters during the ripening and storage of ovine hard-gruyere-type cheese. *Int. Dairy J.* 50, 1–8.
- Noronha, C., Matos, S., Calegari, R., Manique, P., 2014. Characterization of antioxidant methylcellulose film incorporated with  $\alpha$ -tocopherol nanocapsules. *Food Chem.* 159, 529–535.
- Ollé Resa, C., Gerschenson, L., Jagus, R., 2014a. Natamycin and nisin supported on starch edible films for controlling mixed culture growth on model systems and port salut cheese. *Food Contr.* 44, 146–151.
- Ollé Resa, C., Jagus, R., Gerschenson, L., 2014b. Natamycin efficiency for controlling yeast growth in models systems and on cheese surfaces. *Food Contr.* 35 (1), 101–108.
- Ollé Resa, C., Gerschenson, L., Jagus, R., 2016. Starch edible film supporting natamycin and nisin for improving microbiological stability of refrigerated argentinian port salut cheese. *Food Contr.* 59, 737–742.
- Oymaci, P., Altinkaya, S., 2016. Improvement of barrier and mechanical properties of whey protein isolate based food packaging films by incorporation of Zein nanoparticles as a novel bionanocomposite. *Food Hydrocolloids* 54, 1–9.
- Ozer, B., Uz, M., Oymaci, P., Altinkaya, S., 2016. Development of a novel strategy for controlled release of lysozyme from whey protein isolate based active food packaging films. *Food Hydrocolloids* 61, 877–886.
- Pérez-Córdoba, L., Sobral, P.J.A., 2017. Physical and antioxidant properties of films based on gelatin, gelatin-chitosan or gelatin-sodium caseinate blends loaded with nanoemulsified active compounds. *J. Food Eng.* 213, 47–53.
- Pérez-Córdoba, L., Norton, I., Batchelor, H., Gkatzionis, K., et al., 2018. Physico-chemical, antimicrobial and antioxidant properties of gelatin-chitosan based films loaded with nanoemulsions encapsulating active compounds. *Food Hydrocolloids* 79, 544–559.
- Pintado, C., Ferreira, M., Sousa, I., 2010. Control of pathogenic and spoilage microorganisms from cheese surface by whey protein films containing malic acid, nisin, and natamycin. *Food Contr.* 21 (3), 240–246.
- Ramos, Ó., Santos, A., Leão, M., Pereira, J., et al., 2012. Antimicrobial activity of edible coatings prepared from whey protein isolate and formulated with various antimicrobial agents. *Int. Dairy J.* 25 (2), 132–141.
- Ramos, Ó., Reinas, I., Silva, S., Fernandes, J., et al., 2013. Effect of whey protein purity and glycerol content upon physical properties of edible films manufactured therefrom. *Food Hydrocolloids* 30 (1), 110–122.
- Re, R., Pellegrini, N., Proteggente, A., Pannala, A., et al., 1999. Antioxidant activity applying an improved ABTS radical cation decolorization assay. *Free Radic. Biol. Med.* 26 (9), 1231–1237.
- Robertson, G., 2013. *Food Packaging: Principles and Practice*, third ed. Taylor & Francis Group, New York.
- Schmid, M., Pröls, S., Kainz, D., Hammann, F., Grupa, U., 2017. Effect of thermally induced denaturation on molecular interaction-response relationships of whey protein isolate based films and coatings. *Prog. Org. Coating* 104, 161–172.
- Schmid, M., Merzbacher, S., Müller, K., 2018. Time-dependent crosslinking of whey protein based films during storage. *Mater. Lett.* 215, 8–10.
- Shokri, S., Ehsani, A., 2017. Efficacy of whey protein coating incorporated with lactoperoxidase and  $\alpha$ -tocopherol in shelf life extension of pike-perch fillets during refrigeration. *LWT - Food Sci. Technol. (Lebensmittel-Wissenschaft -Technol.)* 85, 225–231.
- Zhao, Y., Lv, X., Ni, H., 2018. Solvent-based separation and recycling of waste plastics: a review. *Chemosphere* 209, 707–720.
- Zhou, X., Hua, X., Huang, L., Xu, Y., 2019. Bio-utilization of cheese manufacturing wastes (cheese whey powder) for bioethanol and specific product (galactonic acid) production via a two-step bioprocess. *Bioresour. Technol.* 272, 70–76.